

2004

Uranium Doping and Thermal Neutron Irradiation Flux Pinning Effects in MgB₂

Tania M. Silver

University of Wollongong, tsilver@uow.edu.au

J. Horvat

University of Wollongong, jhorvat@uow.edu.au

M. Reinhard

ANSTO, Australia

P. Yao

University of Wollongong

S. Keshavarzi

University of Wollongong

See next page for additional authors

Follow this and additional works at: <https://ro.uow.edu.au/engpapers>



Part of the [Engineering Commons](#)

<https://ro.uow.edu.au/engpapers/2>

Recommended Citation

Silver, Tania M.; Horvat, J.; Reinhard, M.; Yao, P.; Keshavarzi, S.; Munroe, P.; and Dou, S. X.: Uranium Doping and Thermal Neutron Irradiation Flux Pinning Effects in MgB₂ 2004.
<https://ro.uow.edu.au/engpapers/2>

Authors

Tania M. Silver, J. Horvat, M. Reinhard, P. Yao, S. Keshavarzi, P. Munroe, and S. X. Dou

Uranium Doping and Thermal Neutron Irradiation Flux Pinning Effects in MgB_2

Tania M. Silver, Joseph Horvat, Mark Reinhard, Pei Yao, Shokat Keshavarzi, Paul Munroe, and Shi Xue Dou

Abstract—The U/n method is a well-established means of improving flux pinning and critical current performance in cuprate superconductors. The method involves the doping of the superconductor with ^{235}U followed by irradiation with thermal neutrons to promote fission. The resultant columnar damage tracks produced by the energetic fission products pin flux vortices and improve critical current performance in magnetic fields. No such improvement could be observed when the U/n method was applied to the MgB_2 superconductor. No fission tracks could be observed in TEM, even for samples that were irradiated at the highest fluence. Gamma-ray spectroscopy indicated that fission had occurred in the expected way. The likely resistance of MgB_2 to the formation of fission tracks is highly relevant to attempts to improve flux pinning and superconducting performance in this material through the introduction of columnar defects.

Index Terms—Flux pinning, MgB_2 , U/n method, uranium doping.

I. INTRODUCTION

SINCE its superconducting properties were first discovered in 2001 [1], [2], MgB_2 has been found to share characteristics with both conventional low-temperature superconductors (LTS) and with cuprate high-temperature superconductors (HTS) [3]. Its critical temperature T_c is nearly 40 K, unusually high for a noncuprate material. Although MgB_2 films have attained critical currents above 10^6 A/cm^2 at 4.2 K in low magnetic fields [4], MgB_2 [3] and the HTS cuprates [5] share a rapidly decreasing $J_c(H)$ performance as magnetic fields increase, compared to LTS superconductors such as Nb_3Sn and Nb-Ti . In HTS materials, the field performance is related to both weak links between grains and poor flux pinning behavior. The former consideration does not apply to MgB_2 , as transport measurements of J_c and measurements calculated from magnetic hysteresis loops yield very similar results, indicating that the flow of supercurrent is not hindered by grain boundaries [6],

[7]. The flux creep in MgB_2 is much weaker than in average HTS [8], [9], indicating stronger vortex pinning. However, this pinning still needs to be improved to offset the effect of the low H_{c2} of MgB_2 (about 18 T) [10] on the field dependence of J_c .

Superconductivity above H_{c1} in any type-II material depends on flux pinning in regions where the superconducting order parameter is reduced, either by intrinsic features of the crystal structure or by point or extended defects. This prevents motion of the flux vortices due to Lorentz forces, resulting in local superconducting phase slip and a nonzero electrical resistance [11]. Strong pinning centers and J_c improvements in HTS superconductors have been produced over the years by means such as the introduction of precipitates and the use of a variety of irradiation techniques employing neutrons, heavy ions, electrons, and protons [5]. Some methods of introducing pinning centers have also been at least partially successful with MgB_2 , including oxygen alloying in thin films [4] and the addition of nanoscale particles of SiC [12] and Si [13], as well as irradiation with protons [14] and neutrons [15], [16].

Heavy ion irradiation is used to introduce columnar defects into HTS materials. Narayan *et al.* [17] irradiated polycrystalline MgB_2 with 200 MeV ^{107}Ag ions. The surfaces of the irradiated samples were imaged with scanning tunneling microscopy (STM), and there was evidence of amorphous tracks 65 Å in diameter. The lengths of the tracks could not be determined, but computer modeling indicated that the ions should penetrate 15 μm into the material. They did not attempt to determine J_c in the irradiated samples. Olsson *et al.* [18], on the other hand, irradiated 4000-Å thick *c*-axis oriented MgB_2 films with 1.2 GeV U^{57+} ions and 1.4 GeV Au^{32+} ions with the beam parallel to the *c* axis. They also examined the surfaces of their irradiated samples with STM and found no evidence of columnar defects in any of the samples. They also found no significant differences in magnetization and, hence, J_c between the irradiated and unirradiated samples. Because a number of parameters are involved, as described below, in determining whether amorphous columnar defects will form in a particular material, the question remains open for MgB_2 .

Another similar irradiation method that has not yet been reported for MgB_2 is the U/n [19], [20] method that is the subject of the present work; although, it has been highly successful in improving flux pinning in HTS. The U/n method differs from straightforward irradiation with thermal neutrons in that the material is first doped with compounds containing ^{235}U . When irradiation takes place the ^{235}U atoms absorb thermal neutrons and fission. The two fission products recoil in opposite directions with a total kinetic energy of approximately 160 MeV, creating extended defects in HTS in the form of two fission tracks.

Manuscript received October 26, 2003. This paper was recommended by Associate Editor J. Willis. This work was supported in part by the Australian Institute of Nuclear Science and Engineering under Award 02/121.

T. M. Silver, J. Horvat, S. Keshavarzi, and S. X. Dou are with the Institute for Superconducting and Electronic Materials (ISEM), Faculty of Engineering, University of Wollongong, Wollongong, NSW 2522, Australia (e-mail: tsilver@uow.edu.au; jhorvat@uow.edu.au; sk78@uow.edu.au; shidou@uow.edu.au).

M. Reinhard is with Safety and Radiation Science, Australian Nuclear Science and Technology Organization (ANSTO), Lucas Heights 2234, Australia (e-mail: mrz@ansto.gov.au).

P. Yao was with the Institute for Superconducting and Electronic Materials (ISEM), University of Wollongong, Wollongong 2522, Australia. He is now with the Centre for Analysis, Tianjin University, Tianjin, China (e-mail: pyao@tju.edu.cn).

P. Munroe is with the Electron Microscopy Unit, University of New South Wales, Sydney 2052, Australia (e-mail p.munroe@unsw.edu.au).

Digital Object Identifier 10.1109/TASC.2004.825384

Fission tracks are made up of amorphous material and are approximately 10 μm long and 10 nm in diameter in Bi-based HTS superconductors [21]. The track structure is discontinuous and randomly oriented.

U/n achieves its greatest success with highly anisotropic Bi-based (BSCCO) superconductors such as Bi-2223 (anisotropy coefficient $\gamma = 31$ [22]), where a 500-fold improvement in J_c was reported for Ag-clad tape [23] at 77 K and 0.8 T for $H//c$. There was also improvement after irradiation for $H//ab$, but J_c improved less than one order of magnitude. The ratio $J_c(H//ab)/J_c(H//c)$ was reduced 23 times at 0.5 T and 77 K. A lesser 20-fold improvement in J_c at 77 K and 0.25 T has been reported [24] in bulk melt textured $\text{YBa}_2\text{Cu}_3\text{O}_{7-\delta}$ (YBCO), which is much less anisotropic ($\gamma = 5$ [25]). This is because the vortices in HTS are two-dimensional (2-D) pancake vortices, residing on the CuO_2 planes [26], [27]. In highly anisotropic HTS, these pancake vortices in each CuO_2 layer can move independently from the vortices in the other CuO_2 layers. However, if the pinning centers are in the shape of long columns traversing the CuO_2 planes, the pancake vortices in different layers will be collectively pinned along these columns and will thus be effectively aligned into vortex lines without an unacceptably high density of defects. Such pinning has been shown to be much more effective than pinning by point-like pinning centers [5].

In MgB_2 , reported results for the anisotropy coefficient $\gamma = \xi_{ab}/\xi_c$ range from 1.1 to 2.7 for textured bulk, aligned crystallites, films, and single crystal [3], [28], indicating that enormous improvements cannot be expected from fission tracks or other columnar defects. There is no evidence of a 2-D vortex state in MgB_2 bulk material, and the I-V characteristics have been reported as consistent with a vortex glass model [29], [30]. However, as with HTS, the reported coherence length values [3] of $\xi_{ab}(0) = 3.7\text{--}12$ nm and $\xi_c(0) = 1.6\text{--}3.6$ nm are of the same order as the expected diameter of the fission tracks introduced by high energy fragments resulting from the fission of ^{235}U . It has been generally accepted that the optimal size of a pinning center is of the order of the coherence length [31].

The most serious problem for the U/n method in MgB_2 is the enormous cross section of 3837 barn (b , where $1b = 10^{-28} \text{ m}^2$) for the $^{10}\text{B}(n, \alpha)^7\text{Li}$ nuclear reaction at thermal (of the order of 25 meV) neutron energies. Here, a ^{10}B nucleus and a neutron react to form an α particle of kinetic energy 1.47 MeV and a ^7Li nucleus with a kinetic energy of 0.84 MeV. By comparison, the ^{235}U fission cross section is 584 b . Natural boron is comprised of 19.9% ^{10}B , with the balance ^{11}B . The $^{10}\text{B}(n, \alpha)^7\text{Li}$ reaction was deliberately used by Babic *et al.* [15] in an attempt to improve flux pinning by introducing ion tracks into MgB_2 . They reported an enhancement in the upper critical field (as did Eisterer *et al.* [16], who also studied neutron irradiation of MgB_2) and an enhancement of magnetization hysteresis loops and hence J_c . However, the distribution of defects was extremely inhomogeneous in both reports because the high content of ^{10}B would have only allowed the neutrons to penetrate into a thin surface layer before being completely absorbed. In using the U/n method, we essentially eliminated the competition for thermal neutrons between ^{10}B and ^{235}U by using highly enriched ^{11}B instead of natural boron. (^{11}B has a total thermal neu-

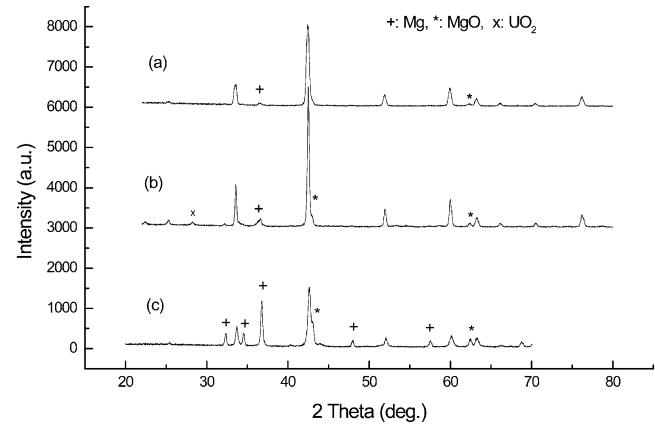


Fig. 1. XRD spectra of the MgB_2 used for the samples. (a) Undoped, sintered at 900 $^{\circ}\text{C}$ for 3 h; (b) doped with 1 wt% U as UO_2 , sintered at 900 $^{\circ}\text{C}$ for 3 h; and (c) undoped, sintered at 760 $^{\circ}\text{C}$ for 0.5 h. MgB_2 phase peaks are unmarked.

tron cross section of 5.05 b , almost all of it representing elastic scattering.) The negative results we describe below thus strongly support the position of [18] since they cannot be attributed to self-shielding effects.

II. EXPERIMENT

To test the applicability of the U/n technique for enhancing J_c in MgB_2 , an experimental program was designed. Powders of 1–11 μm Mg from Hypertech (for samples A–D) or 325 mesh Mg (for sample E) and crystalline B (99.5 at% ^{11}B , particle size $< 22 \mu\text{m}$, from Eagle-Picher) were mixed in a mortar in a stoichiometric atomic ratio of 1:2. Half of the powders were mixed with UO_2 (93% enriched in ^{235}U) to give 1 wt% U. Optical microscopy revealed that the UO_2 particles ranged from 2–4 μm in diameter.

The powders were pressed into 0.4 g pellets and the pellets sealed in iron tubes. Sintering took place in a tube furnace under flowing argon. For samples A–D the temperature was ramped up to 760 $^{\circ}\text{C}$ over 1 h. The pellets were held at that temperature for 30 min and then furnace cooled. For sample E, the temperature was ramped up to 900 $^{\circ}\text{C}$ over 1.5 h, and the pellets were held at that temperature for 3 h, then furnace cooled. The densities of the samples were 1.4 g/cm^3 (samples A–D) and 1.0–1.1 g/cm^3 (sample E). X-ray diffraction (XRD) was used to determine the phase composition of the doped and undoped samples, while energy dispersive spectroscopy (EDS) was used to determine the uranium distribution of doped samples. Portions of the doped and undoped samples were then cut and filed into small regular rectangular blocks with dimensions of typically $3\text{--}4 \times 3 \times 2 \text{ mm}^3$. The magnetization and ac susceptibility were determined using a quantum design physical properties measurement system (PPMS) in a time-varying magnetic field with sweep rate 50 Oe/s and amplitude up to 8.5×10^4 Oe, with the applied magnetic field parallel to the longest dimension of the sample. The low-field zero field cooled (ZFC) and field cooled (FC) measurements were made with a quantum design magnetic properties measurement system (MPMS). The J_c values at different magnetic fields and temperatures were calculated from the height ΔM of the magnetic hysteresis loops using the Bean model: $J_c = 20\Delta M/[a(1 - a/3b)]$, where a

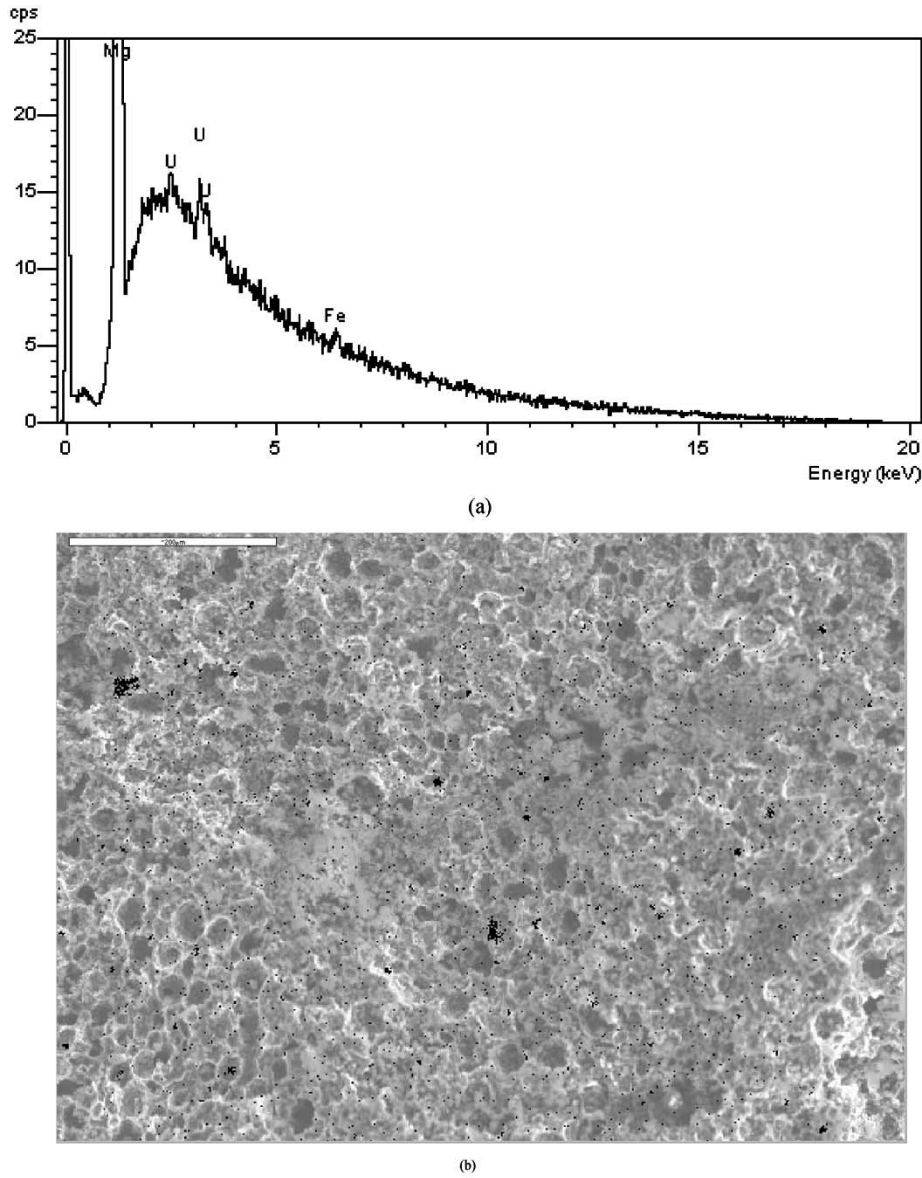


Fig. 2. (a) Averaged EDS spectrum of sample E doped with 1 wt% uranium. (b) EDS mapping of a cross-sectional area of sample E showing the distribution of the UO_2 particles in black.

and b are the dimensions of the sample perpendicular to the applied field, $a < b$. T_c was determined from the ac susceptibility measurements.

Small block samples, in doped and undoped pairs, were double encapsulated in titanium capsules and irradiated by neutrons in HIFAR, a 10-MW DIDO class research reactor operated by ANSTO at Lucas Heights, Australia. The irradiation rig was located within the graphite region of the reactor, and thus the neutron energy spectrum was highly thermalized with only a minimal fast and epithermal neutron component. The rig was rated with a nominal neutron flux of $\sim 1 \times 10^{13} \text{ cm}^{-2}\text{s}^{-1}$. Four different fluences were used: $2 \times 10^{16} \text{ cm}^{-2}$ (A), $5 \times 10^{15} \text{ cm}^{-2}$ (B,E), $5 \times 10^{14} \text{ cm}^{-2}$ (C), and $5 \times 10^{13} \text{ cm}^{-2}$ (D). Following irradiation, the J_c and flux pinning properties of the irradiated pellets were then compared with the pre-irradiated results. The doped irradiated samples were examined by TEM to detect any fission tracks and the extent of fission determined by gamma ray spectroscopy.

III. RESULTS AND DISCUSSION

XRD using a Philips 1730 phase XRD diffractometer showed that greater phase purity could be obtained using the longer, hotter sintering to fully react the crystalline boron and the magnesium (see Fig. 1). After 3 h at 900 °C, the sintered undoped sample E material (a) is MgB_2 with traces of Mg and MgO. The sintered 1wt% U-doped sample E material (b) also consists of MgB_2 with traces of Mg, MgO, and UO_2 . Fig. 1(c) shows the undoped sintered material characteristic of samples A-D. Because the sintering was shorter and at a lower temperature the Mg and MgO impurity contents are much higher, due to the much larger amount of remaining unreacted crystalline boron. These short sintering conditions are appropriate when amorphous boron is used to make MgB_2 . The impurities would be expected to give a smaller superconducting volume, but the intragranular properties affected by the U/n method would not be degraded.

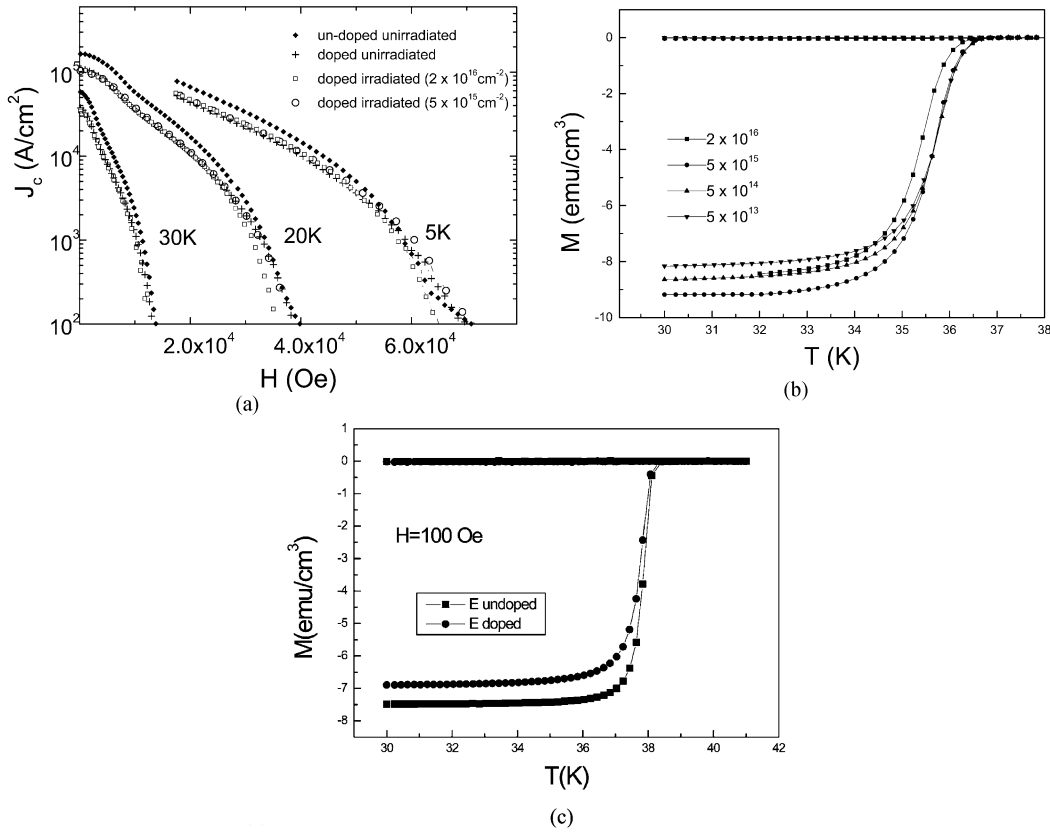


Fig. 3. (a) Critical current derived from PPMS measurements as a function of magnetic field at 5, 20, and 30 K for sample A (undoped and doped with 1 wt% U). J_c for the doped version of sample A is shown before and after irradiation at 2×10^{16} cm⁻² with thermal neutrons. J_c for the doped version of sample B (also 1 wt% U) is shown after irradiation with thermal neutrons at 5×10^{15} cm⁻². Low field 5-K data is not shown as it is affected by flux jumping. (b) Magnetization under ZFC and FC conditions as a function of temperature at a field of 100 Oe as determined by MPMS measurements. All the samples shown were doped to 1 wt% U and irradiated at the fluences/cm² that are shown in the legend. (c) MPMS measurements under the same conditions for the unirradiated high purity sample E, both undoped and doped to 1 wt% U.

Samples were characterized using a Cambridge Leica scanning electron microscope (SEM) equipped with an energy dispersive spectrometer (EDS). The results showed MgB₂ grains in a porous structure. The UO₂ particles remained separate, and the larger agglomerates could be distinguished at the grain boundaries. EDS analysis revealed the presence of large amounts of Mg and small amounts of U and Fe, the source of which was most likely the iron tubing containing the samples during sintering. The boron could not be detected with the experimental setup. Fig. 2(a) shows an EDS spectrum of the doped version of sample E. Fig. 2(b) shows an EDS map that reveals a reasonably even distribution of UO₂ particles among the MgB₂ grains.

The ac susceptibility of the samples was measured at temperatures from 5 to 45 K and the magnetization from 5 to 30 K using a physical properties measurement system.¹ T_c was determined from the ac susceptibility and was not found to be significantly affected by irradiation and doping. T_c was measured to be 38.5 K with a sharp transition for the higher quality sample E, regardless of doping and approximately 37.2 K for the other samples. The discrepancy is probably because samples A-D have a greater concentration of nonmagnetic impurities, which are known to depress T_c in MgB₂ [32]. Fig. 3(a) shows the derived values of the critical current at 5, 20, and 30 K as a function of magnetic field for three versions of sample A [1] undoped and

unirradiated; 2) doped with 1 wt% U, but not irradiated; and 3) the same piece of doped sample A after irradiation with thermal neutrons at 2×10^{16} cm⁻² and for sample B (doped with 1% U, then irradiated with thermal neutrons at 5×10^{15} cm⁻²). J_c values for sample E were similar, with a slightly lower H_{irr} , probably because the lower density cancelled out any benefits due to the higher purity. It was impossible to accurately determine J_c at 5 K for very low fields because of the presence of thermal flux jumping [33]. J_c performance is slightly worse in the doped samples except at high magnetic fields, probably due to the presence of the additional impurities, but there are no significant differences between the irradiated and unirradiated samples, in contrast to what has been demonstrated for HTS superconductors. The slightly worse performance of the high fluence irradiated sample A at high fields may be due to excessive radiation-induced defects from the higher neutron fluence. Fig. 3(b) shows the ZFC-FC results at 100 Oe as a function of temperature for the doped irradiated versions of samples A-D. There are no significant differences with fluence. Fig. 3(c) shows the preirradiation ZFC-FC results for the doped and undoped versions of sample E. The higher T_c is attributed to the greater phase purity.

TEM was performed on two specimens (A and B) doped to 1 wt% U and irradiated to neutron fluences of 2×10^{16} cm⁻² and 5×10^{15} cm⁻² respectively. For both materials the microstructure was similar, that is, there were grains of MgB₂

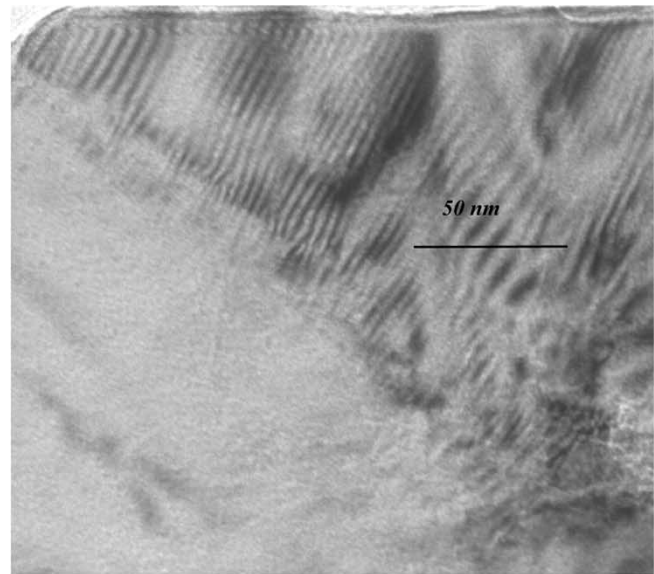
¹Quantum Design, San Diego, CA.

several microns in diameter in which a number of dislocations and other crystalline defects were evident, but no fission tracks. Many such grains were examined under different imaging conditions, and Fig. 4(a) shows a typical example. This observation is in contrast to TEM studies of U-doped Bi-based HTS specimens exposed to similar levels of irradiation, in which the fission tracks appear as straight randomly oriented black lines due to the greater electron scattering from the amorphous material they contain. These fission tracks are several microns in length and clearly visible in TEM even at modest magnifications. This is illustrated in Fig. 4(b), which shows a TEM image of the core of an irradiated uranium-doped Bi-2223/Ag tape.

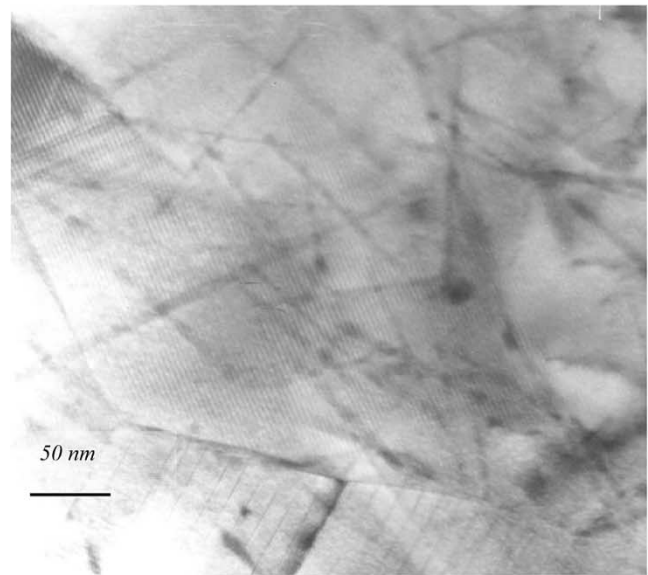
A quantitative analysis of ^{235}U fissions in the present MgB_2 samples was obtained from the fission product yield as measured by the gamma-ray spectrometric method [34]. Measurements were limited to the doped irradiated versions of samples C and D. A period of 92 days had expired since irradiation, which meant that most of the short-lived radioisotopes had decayed. This simplified the spectrum. To facilitate measurements, samples were placed 10 cm from the face of a large volume coaxial high purity germanium (HPGe) detector. The gamma ray spectrum for sample C is shown in Fig. 5. The spectral features were consistent with a 96 day decayed ^{235}U fission product spectrum [35]. The actual fission yield (see Table I) was determined from the measured ^{137}Cs activity and the cumulative fission yield data for ^{137}Cs from ^{235}U . The cumulative yield includes the total number of ^{137}Cs atoms produced directly as a result of fission in addition to ^{137}Cs atoms produced via radioactive decay of the ^{137}Cs precursors, namely ^{137}I and ^{137}Xe , which both have half-lives of less than 5 min. By comparison, the half-life of ^{137}Cs is 30.17 years. The ^{137}Cs activity was determined from the peak area of the 662-keV emission and the known detector efficiency at this energy.

The fission yield can also be estimated from knowledge of the sample ^{235}U content, the cross section for fission of ^{235}U , and the neutron fluence. The estimated fission yield along with the results from the gamma-ray spectrometric method is given in Table I. A good correlation between estimated and measured fission yield was obtained. This shows that nuclear fission of ^{235}U did occur as expected. In HTS, the same fission would produce columnar defects [Fig. 4(b)], resulting in strong pinning improvement. However, not a single fission track was observed for MgB_2 [Fig. 4(a)], and the field dependence of J_c was virtually unchanged after the irradiation [Fig. 3(a)].

In our experiments, heavy ions of about 80 MeV are created by the nuclear fission and transfer their energy to the MgB_2 . The occurrence or otherwise of the fission tracks can be described by the thermal spike model [36]–[38]. Because of the transfer of energy from the heavy ions to the electrons and subsequently to the crystal lattice on a longer time scale, a sudden localized increase in temperature occurs along the ion path through the crystal. For values of the electronic stopping power S_e [39] higher than the threshold value S_{e0} [40], which is dependent on the target material and fission products, the crystal lattice melts in a very localized volume along the ion track. Because the diameter of the molten volume is very small (of the order of a nanometer), this heat is diffused through the crystal lattice quickly enough to freeze the molten volume without allowing recrystallization.



(a)



(b)

Fig. 4. (a) Typical TEM image of an MgB_2 grain from sample B (doped to 1 wt% U and irradiated at $5 \times 10^{15} \text{ cm}^{-2}$ with thermal neutrons). This grain, like all the others examined, shows no evidence of columnar defects that might be due to fission tracks. (b) TEM image of the core of a U-doped irradiated Bi-2223/Ag tape showing fission tracks.

Consequently, a track of amorphous material is formed in the crystal, which is not superconducting and is expected to be a strong pinning center. In our experiments, there was no evidence for the formation of fission tracks. The reason for this may be that the S_e values were too low for the array of fission products interacting with MgB_2 , or that the heat conductivity required for freezing the molten volume is too low in MgB_2 , or that the energy transfer from the ions to the crystal electrons and the crystal lattice does not occur on timescales that would enable melting of the lattice. Thus, many parameters, currently unknown for MgB_2 , are required to predict the presence or absence of amorphous tracks.

It is interesting to compare our results with experiments that employed 2 MeV proton irradiation [14] in order to improve

TABLE I
COMPARISON OF ^{235}U FISSION YIELD ESTIMATED PRIOR TO IRRADIATION AND MEASURED AFTER IRRADIATION USING THE GAMMA-RAY SPECTROMETRIC TECHNIQUE

Sample	^{235}U fission yield (Calculated)	^{235}U fission yield (Gamma spectrometric method)
C	1.93×10^{11}	1.06×10^{11}
D	2.31×10^{10}	3.04×10^{10}

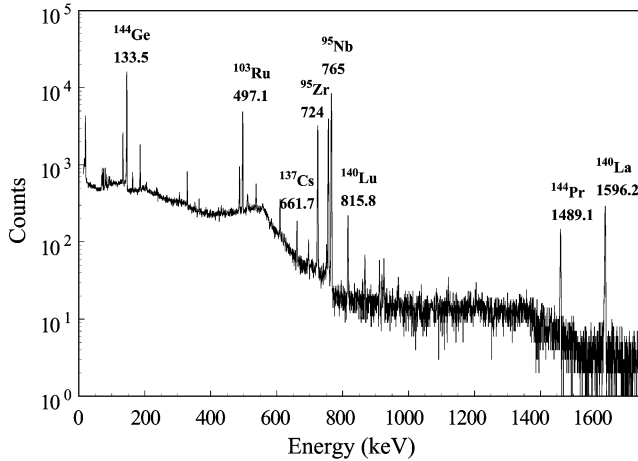


Fig. 5. Gamma ray spectrum of sample C (doped to 1 wt% U and irradiated to a fluence of $5 \times 10^{15} \text{ cm}^{-2}$) 92 days after neutron irradiation.

vortex pinning in MgB_2 . There, an improvement in the field dependence of J_c and the irreversibility field was observed. It is likely that the 2 MeV protons used in [14] were producing point defects in MgB_2 , which are much weaker pinning centers than columnar defects. However, due to the very large density of defects introduced, an observable increase of J_c was obtained. Point defects are also likely to be responsible for the improvements reported in [15] due to the $^{10}\text{B}(n, \alpha)^7\text{Li}$ nuclear reaction, rather than any ion tracks.

The relevance of this paper to research in superconductivity is that it shows that uranium fission fragments probably cannot be used for the introduction of columnar defects in MgB_2 . This research also identifies the need to obtain the values of the parameters affecting the formation of columnar defects in MgB_2 , if some other method for the introduction of columnar defects is to be devised. It also shows that previously published results on the introduction of pinning centers with high-energy particles have to be taken with caution, because it is highly questionable if columnar defects were introduced in such a way.

ACKNOWLEDGMENT

The authors would like to thank X. L. Wang, K. Konstantinov, A. Pan, M. J. Qin, M. Ionescu, and B. R. Winton of the Institute for Superconducting and Electronic Materials and D. Wexler of the Faculty of Engineering, University of Wollongong, for practical help and useful discussions.

REFERENCES

- [1] J. Akimitsu, 2002 *Symp. Transition Metal Oxides*, Sendai, Japan, Jan. 10, 2001.
- [2] J. Nagamatsu, J. Nakagawa, T. Muranaka, Y. Zenitani, and J. Akimitsu, "Superconductivity at 39 K in magnesium diboride," *Nature*, vol. 410, p. 63, 2001.
- [3] C. Buzea and T. Yamashita, "Review of the superconducting properties of MgB_2 ," *Supercond. Sci. Technol.*, vol. 14, p. R115, 2001.
- [4] C. B. Eom, M. K. Lee, J. H. Choi, L. J. Belenky, X. Song, L. D. Cooley, M. T. Naus, S. Patnaik, J. Jiang, M. Rikel, A. Polyanskii, A. Gurevich, X. Y. Cai, S. D. Bu, S. E. Babcock, E. E. Hellstrom, D. C. Larbalestier, N. Rogado, K. A. Regan, M. A. Hayward, T. He, J. S. Slusky, K. Inamaru, M. K. Haas, and R. J. Cava, "High critical current density and enhanced irreversibility field in superconducting MgB_2 thin films," *Nature*, vol. 411, p. 558, 2001.
- [5] M. E. McHenry and R. A. Sutton, "Flux pinning and dissipation in high temperature oxide superconductors," *Progress Mater. Sci.*, vol. 38, p. 159, 1994.
- [6] K. H. P. Kim, W. N. Kang, M. S. Kim, C. U. Jung, H. J. Kim, E. M. Choi, M. S. Park, and S. I. Lee, "Negligible effect of grain boundaries on the supercurrent density in polycrystalline MgB_2 ," *Phys. C*, vol. 370, p. 13, 2002.
- [7] Y. Bugoslavsky, G. K. Perkins, X. Qi, L. F. Cohen, and A. D. Caplin, "Vortex dynamics in superconducting MgB_2 and prospects for applications," *Nature*, vol. 410, p. 563, 2001.
- [8] H. H. Wen, S. L. Li, Z. W. Zhao, H. Jin, Y. M. Ni, W. N. Kang, H. J. Kim, E. M. Choi, and S. I. Lee, "Magnetic relaxation and critical current density of MgB_2 thin films," *Phys. Rev. B*, vol. 64, p. 134 505, 2001.
- [9] H. H. Wen, S. L. Li, Z. W. Zhao, H. Jin, Y. M. Ni, Z. A. Ren, G. C. Che, and Z. X. Zhao, "Flux dynamics and vortex phase diagram of the new superconductor MgB_2 ," *Phys. C*, vol. 363, p. 170, 2001.
- [10] D. C. Larbalestier, L. D. Cooley, M. O. Rikel, A. A. Polyanskii, J. Jiang, S. Patnaik, X. Y. Cai, D. M. Feldmann, A. Gurevich, A. A. Squitieri, M. T. Naus, C. B. Eom, E. E. Hellstrom, R. J. Cava, K. A. Regan, N. Rogado, M. A. Hayward, T. He, J. S. Slusky, P. Khalifah, K. Inamaru, and M. Haas, "Strongly linked current flow in polycrystalline forms of the superconductor MgB_2 ," *Nature*, vol. 410, p. 186, 2001.
- [11] D. S. Fisher, M. P. A. Fisher, and D. A. Huse, "Thermal fluctuations, quenched disorder, phase transitions, and transport in type-II superconductors," *Phys. Rev. B*, vol. 43, p. 130, 1991.
- [12] S. X. Dou, S. Soltanian, J. Horvat, X. L. Wang, S. H. Zhou, M. Ionescu, and H. K. Liu, "Enhancement of the critical current density and flux pinning of MgB_2 superconductor by nanoparticle SiC doping," *Appl. Phys. Lett.*, vol. 81, p. 3419, 2002.
- [13] X. L. Wang, S. H. Zhou, M. J. Qin, P. R. Munroe, S. Soltanian, H. K. Liu, and S. X. Dou, "Significant enhancement of the flux pinning in MgB_2 superconductor through nano-Si addition," *Phys. C*, vol. 385, p. 461, 2003.
- [14] Y. Bugoslavsky, L. F. Cohen, G. K. Perkins, M. Polichetti, T. J. Tate, R. Gwillam, and A. D. Caplin, "Enhancement of the high-magnetic field critical current density of superconducting MgB_2 by proton irradiation," *Nature*, vol. 411, p. 561, 2001.
- [15] E. Babic, B. Miljanic, K. Zadro, I. Kusevic, Z. Marohnic, D. Drobac, X. L. Wang, and S. X. Dou, "Enhancement of flux pinning in neutron irradiated MgB_2 superconductor," *Fizika A*, vol. 10, p. 87, 2001.
- [16] M. Eisterer, M. Zehetmayer, S. Tonies, and H. W. Weber, "Neutron irradiation of MgB_2 bulk superconductor," *Supercond. Sci. Technol.*, vol. 15, p. L9, 2002.
- [17] H. Narayan, S. B. Samanta, A. Gupta, A. V. Narlikar, R. Kishore, K. N. Sood, D. Kanjilal, T. Muranaka, and J. Akimitsu, "SEM, STM/STS and heavy ion irradiation studies on magnesium diboride superconductor," *Phys. C*, vol. 377, p. 1, 2002.
- [18] .
- [19] R. Weinstein, Y. Ren, J. Liu, I. Chen, R. Sawh, C. Foster, and C. Obot, *Proc. Int. Symp. Superconductivity, Hiroshima, 1993*, Springer, Berlin, Germany, 1993, p. 285.
- [20] G. W. Schulz, C. Klein, H. W. Weber, S. Moss, R. Zeng, S. X. Dou, R. Sawh, Y. Ren, and R. Weinstein, "Enhancement of transport critical current densities in $\text{Bi}_2\text{Sr}_2\text{Ca}_2\text{Cu}_3\text{O}_x$ tapes by fission tracks," *Appl. Phys. Lett.*, vol. 73, p. 3935, 1998.
- [21] S. Tönies, H. W. Weber, Y. C. Guo, S. X. Dou, R. Sawh, and R. Weinstein, "On the current transport limitations in Bi-based high temperature superconducting tapes," *Appl. Phys. Lett.*, vol. 78, p. 3851, 2001.

- [22] I. Matsubara, H. Tanigawa, T. Ogura, H. Yamashita, M. Kinoshita, and T. Kawai, "Uppercritical field and anisotropy of the high- T_c $\text{Bi}_2\text{Sr}_2\text{Ca}_2\text{Cu}_3\text{O}_x$ phase," *Phys. Rev. B*, vol. 45, p. 7414, 1992.
- [23] S. X. Dou, Y. C. Guo, D. Marinaro, J. W. Boldeman, J. Horvat, P. Yao, R. Weinstein, A. Gandini, R. Sawh, and Y. Ren, "The effects of uranium doping and thermal neutron irradiation on the pinning properties of Ag/Bi-2223 tapes," *IEEE Trans. Appl. Supercond.*, vol. 11, p. 3896, 2001.
- [24] M. Eisterer, S. Tönies, H. W. Weber, R. Weinstein, R. Sawh, and Y. Ren, "High critical currents due to fission tracks in $\text{Yb}_{1-x}\text{Ba}_x\text{Cu}_3\text{O}_{7-\delta}$," *Phys. C*, vol. 341–348, p. 1439, 2000.
- [25] T. K. Worthington, W. J. Gallagher, and T. R. Dinger, "Anisotropic nature of high-temperature superconductivity in single-crystal $\text{Y}_1\text{Ba}_2\text{Cu}_3\text{O}_{7-x}$," *Phys. Rev. Lett.*, vol. 59, p. 1160, 1987.
- [26] J. R. Clem, "Two-dimensional vortices in a stack of thin superconducting films—A model for high-temperature superconducting multilayers," *Phys. Rev. B*, vol. 43, p. 7837, 1991.
- [27] —, "Phenomenological theory of magnetic structure in the high-temperature superconductors," *Phys. C*, vol. 162–164, p. 1137, 1989.
- [28] M. B. Maple, B. J. Taylor, N. A. Frederick, S. Li, V. F. Nesterenko, S. S. Indrakanti, and M. P. Maley, "Critical scaling and flux dynamics in bulk MgB_2 and high-purity $\text{Yb}_{1-x}\text{Ba}_x\text{Cu}_3\text{O}_{7-\delta}$ single crystals," *Phys. C*, vol. 382, p. 132, 2002.
- [29] S. K. Gupta, S. Sen, A. Singh, D. K. Aswal, J. V. Yakhmi, E. M. Choi, H. J. Kim, K. H. P. Kim, S. Choi, H. S. Lee, W. N. Kang, and S. I. Lee, "I-V characteristic measurements to study the nature of the vortex state and dissipation in MgB_2 thin films," *Phys. Rev. B*, vol. 6610, p. 4525, 2002.
- [30] N. Takezawa and K. Fukushima, "Optimal size of an insulating inclusion acting as a pinning center for magnetic flux in superconductors: Calculation of pinning force," *Phys. C*, vol. 290, p. 31, 1997.
- [31] "Eur. Phys. J. B," vol. 30, 2002.
- [32] S. X. Dou, X. L. Wang, J. Horvat, D. Milliken, A. H. Li, K. Konstantinov, E. W. Collings, M. D. Sumption, and H. K. Liu, "Flux jumping and a bulk-to-granular transition in the magnetization of a compacted and sintered MgB_2 superconductor," *Phys. C*, vol. 361, p. 79, 2001.
- [33] "Compilation and evaluation of fission yield nuclear data," IAEA, IAEA-TECDOC-1168, 2000.
- [34] R. L. Heath, "Gamma-Ray Spectrum Catalog," ANCR-1000-2.
- [35] G. Szenes, "General feature of latent track formation in magnetic insulators irradiated with swift, heavy ions," *Phys. Rev. B*, vol. 51, p. 8026, 1995.
- [36] F. Seitz and J. F. Koehler, *Solid State Physics: Advances in Research and Applications*, F. Seitz and D. Turnbull, Eds. New York: Academic, 1995, vol. 2, p. 305.
- [37] M. Toulemonde, C. Dufour, and E. Paumier, "Transient thermal process after a high-energy heavy-ion irradiation of amorphous metals and semiconductors," *Phys. Rev. B*, vol. 46, p. 14 362, 1992.
- [38] Y. Zhu, Z. X. Cai, R. C. Budhani, M. Suenaga, and D. O. Welch, "Structures and effects of radiation damage in cuprate superconductors irradiated with several-hundred-MeV heavy ions," *Phys. Rev. B*, vol. 48, p. 6436, 1993.
- [39] J. Provost, Ch. Simon, M. Hervieu, D. Groult, V. Hardy, F. Studer, and M. Toulemonde, "Swift, heavy ions in insulating and conducting oxides: Tracks and physical properties," *Mater. Res. Soc. Bulletin*, vol. 20, p. 22, 1995.
- [40] **Tania M. Silver** Photograph and biography not available at the time of publication.
- Joseph Horvat** Photograph and biography not available at the time of publication.
- Mark Reinhard** Photograph and biography not available at the time of publication.
- Pei Yao** Photograph and biography not available at the time of publication.
- Shokat Keshavarzi** Photograph and biography not available at the time of publication.
- Paul Munroe** Photograph and biography not available at the time of publication.
- Shi Xue Dou** Photograph and biography not available at the time of publication.